SMAR 2017 – Fourth Conference on Smart Monitoring,
Assessment and Rehabilitation of Civil Structures

SMAR 2017

Efforts to develop resilient reinforced concrete building structures in Japan

Susumu Kono[1], Fuhito Kitamura[1], Eko Yuniarsyia[1], Hidekazu Watanabe[2], Tomohisa Mukai[2], and David J. Mukai[3]

[1] Tokyo Institute of Technology, Yokohama, Japan
[2] Building Research Institute, Tsukuba, Japan
[3] University of Wyoming, Laramie, USA

ABSTRACT: Since the 1994 Northridge Earthquake and 1995 Kobe Earthquake, various earthquakes in urban areas have been warning us the importance of resilient building structures. In Japan, resilience of building structures means low or no damage to structural and non-structural members and quick recovery of building functions. In order to achieve resilient building structures, it is important to develop low damage structural systems in a broader sense and propose design procedures. As an economical and easy solution, moment resisting reinforced concrete frame systems strengthened with walls is proposed to achieve both higher lateral load carrying capacity and smaller interstory drift ratios. Based on the proposal, two real scale five-story reinforced concrete buildings were designed and tested in the Building Research Institute in Japan in order to evaluate seismic performance including damage to structural and non-structural members. An experimental work showed that strengthened moment resisting frame have improved performance for damage reduction. In order to simulate crack conditions for the proposed structural system, results of finite element analysis were post-processed to successfully simulate detailed features of flexural cracks such as spacing, width, and length.

1 INTRODUCTION

After the 1994 Northridge Earthquake and 1995 Kobe Earthquake, earthquakes in urban areas caused various degree of damages to reinforced concrete buildings and the concept of resiliency started to attract attentions. Even if buildings had minor structural damages, intermediate to severe damages to non-structural members often lead to interruption of post-earthquake functionality and sometime resulted in demolition. Nowadays, damage to non-structural members are as important as that to structural members from the view point of continuous post-earthquake functionality and resiliency. Practicing engineers and researchers started to work seriously in this area. Resilience of building structures specifically means low or no damage of structural and non-structural members and quick recover of functions of buildings. In order to achieve resilient building structures, it is important to develop low damage structural systems in a broader sense and propose design procedures. Base isolation is one of the good choices but excluded from discussion here for pursuing simpler structural systems.

Damage reduction may be easily achieved by strengthening the whole structure by properly providing reinforced concrete walls. S strength enhancement with ductile detailed walls may be the easiest and most economical solutions. Another way of damage reduction is low damage structural systems such as self-centering rocking walls. Self-centering rocking walls are ductile systems which suffer very little structural damage since deformation of structures concentrates on interfaces between structural components. With these two extreme systems (strong system and ductile system), designers may choose among strong systems, ductile systems, or system in-between to achieve much smaller damage level. All these systems are termed low damage system in a broader sense and very important to achieve resiliency. This paper especially describes the effort of crack evaluation of reinforced concrete members using a real scale building test and numerical analysis since this is one of unique research efforts on resilient reinforced concrete structures in Japan. Crack simulation under seismic loading has been conducted by several researchers in Japan (Maeda et al. 2004, Sato and Naganuma 2011). Their experimental work dealt with scaled model beams and columns and their simulation model has not been validated with real scale building members.

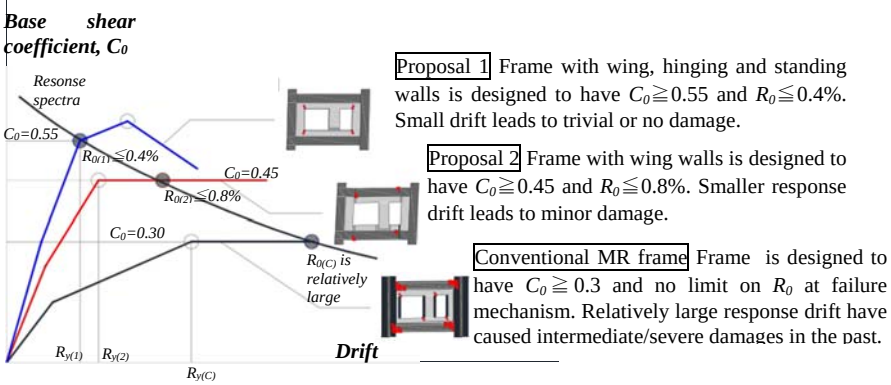

Figure 1. Design philosophy of proposed frames and conventional frame (Fukuyama et al. 2015)

Design philosophy of two proposed methods and conventional method is shown in

Figure 1 (Fukuyama et al. 2015). The current design code (MLIT 2015) requires moment resisting reinforced concrete frame buildings to possess load carrying capacity equivalent to base shear coefficient (C_0) of 0.3 or higher when the building reaches its failure mechanism under code specified static seismic load conditions. This type of typical moment resisting frame

buildings is expressed as conventional moment resisting (MR) frame. Proposed concrete frames have higher load carrying capacity by adding wing walls to columns, or standing or/and hanging walls to beams. Proposal 1 and 2 have load carrying capacity equivalent to C_0=0.45 and 0.55, respectively. Two cases aim at limiting interstory drift, R_0, as small as 0.4% and 0.8% at the time of failure mechanism formation. This implies that Proposal 1 has an elastic response even under large scale earthquakes for no or minor damage. Requirements for Proposal 2 are in-between those for conventional MR frame and Proposal 1 to achieve intermediate damage with lower cost. In addition to dramatic damage decrease to columns and beams, damage to beam-column connections also greatly decreases due to limited deformation. Even if wing walls are damaged due to unexpectedly large interstory drift, columns would continue to carry axial load and collapse of buildings would be prevented. The Building Research Institute in Japan designed and tested two real scale five story reinforced concrete buildings to see seismic performance of two proposed systems. The first building was designed based on Proposal 2 and tested in 2014 (Kabeyasawa et al. 2016 and 2017). The features of cracks of this specimen are discussed from a numerical view point in this paper.

2 EXPERIMENTAL WORK

Figure 2 shows configuration of five story specimen and Figure 3 shows typical section size with reinforcement arrangement and location of displacement gages. Cracks were traced and copied to transparencies and the maximum crack width for each crack was recorded as in Figure 4 and Figure 5.

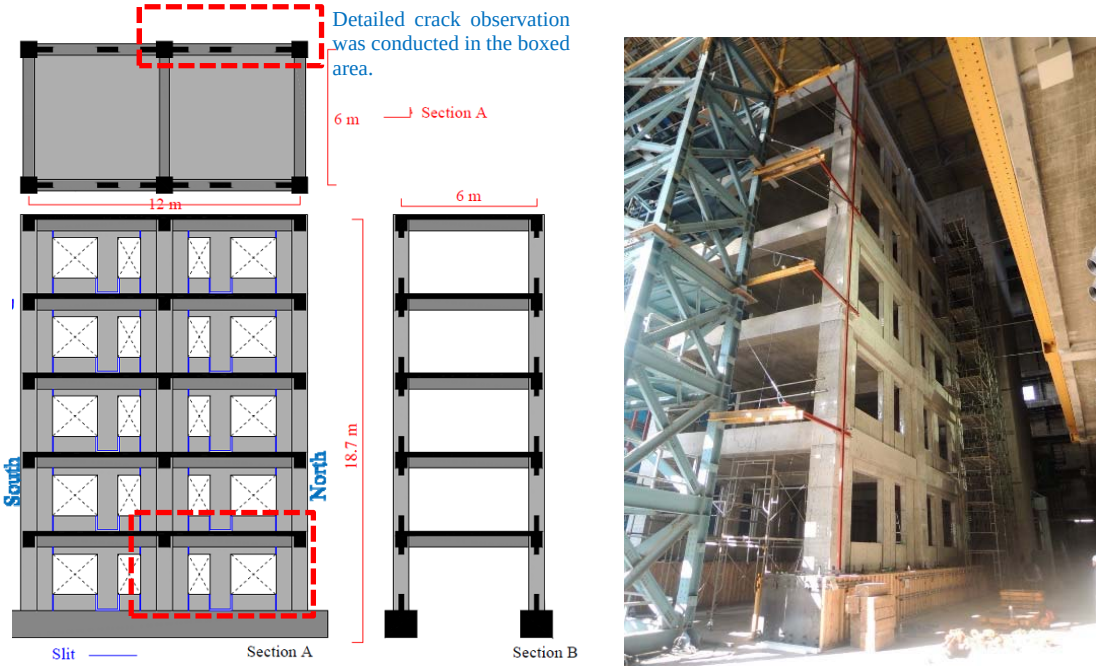

(a) Specimen configuration (b) South east corner of the 2014 specimen

Figure 2. Configuration of the 2014 five story specimen (Fukuyama et al. 2015)

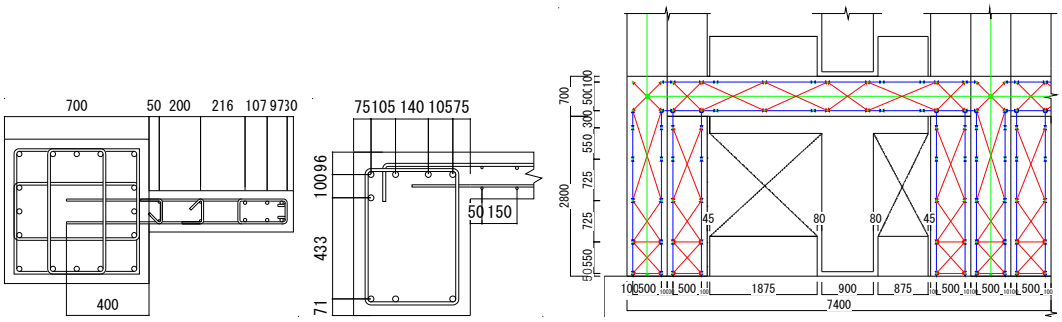

(a) Column with a wing wall (b) Beam with one side slab (c) Displacement gage arrangement (1F)
Figure 3. Typical section size and reinforcement arrangement (Kitamura 2017)

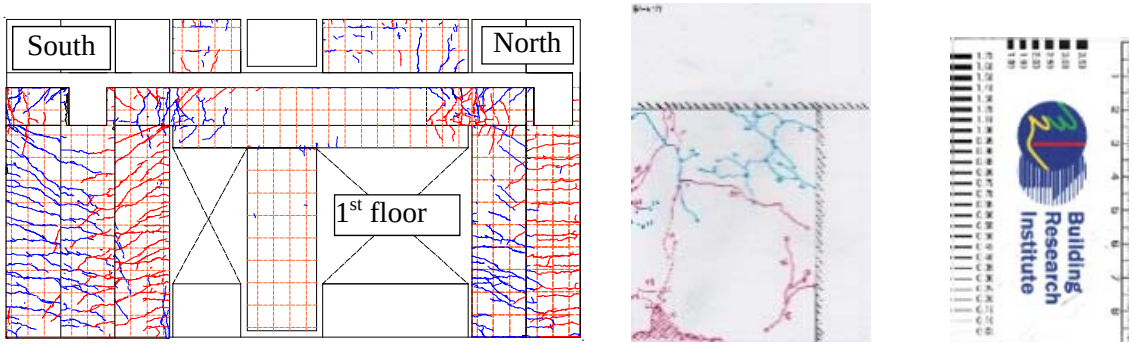

(a) Grid and crack distributions at R=1% (b) Transparency (c) Imprinted crack gage
Figure 4. Measurement of cracks (Kitamura 2017)

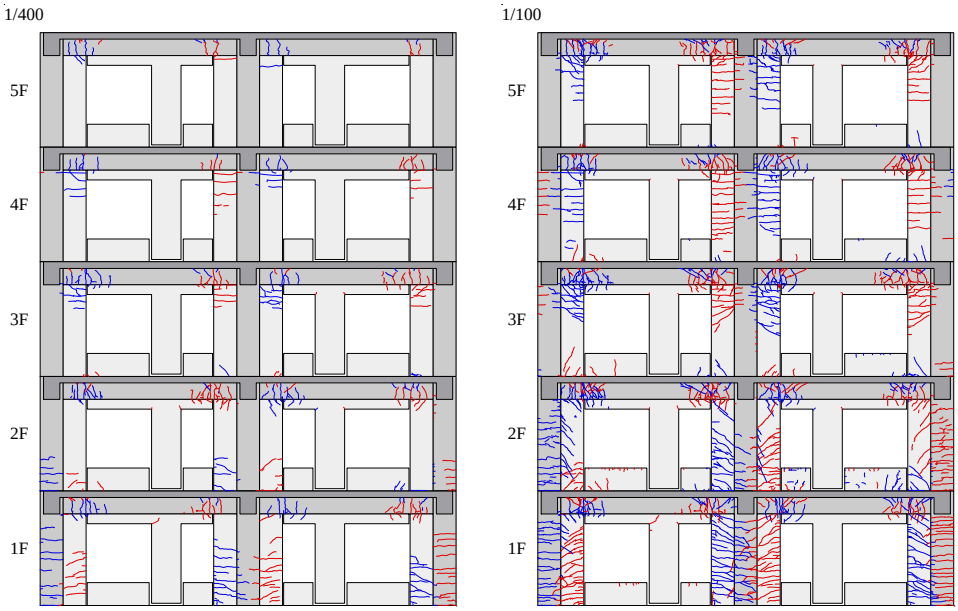

(a) *R*=0.25% (b) *R*=1.0%
Figure 5. Recorded cracks and spalling (Kabeyasawa et al. 2016)

3 SIMULATION OF FLEXURAL CRACKS

3.1 Numerical analysis with an FEM program

Figure 6 shows a 2D finite element mesh used in a commercial FEM program "FINAL" (ITOCHU 2016). Concrete was modeled as isoparametric quadrilateral elements with smeared reinforcement, and longitudinal reinforcement was modeled as beam-column elements. Perfect bond was assumed for all reinforcement. All degrees of freedom of nodes on the bottom face of the foundation beams were fixed. Self-weight was applied as concentrated load at beam-column connections based on a tributary area. Lateral load was applied at the central beam-column connections of roof and fourth floor by 1:2 ratio to simulate the load conditions in experiment. Load was controlled by the lateral displacement of the roof level and loading protocol followed the measured displacement although the second cycle was skipped to save computational time. The numerical simulation was carried out up to R=1% since the resisting mechanism of building changed when construction gaps closed at R=1.3% in experiment. The elements employed default material models of concrete; modified Ahmad model (Naganuma 1995) and Izumo model (Izumo et al. 1987), and reinforcement; modified Menegotto-Pinto model (Ciampi et al. 1982). The detail is described in the master thesis (Kitamura 2017). Numerical analysis employed mechanical properties of concrete and reinforcement obtained in material tests.

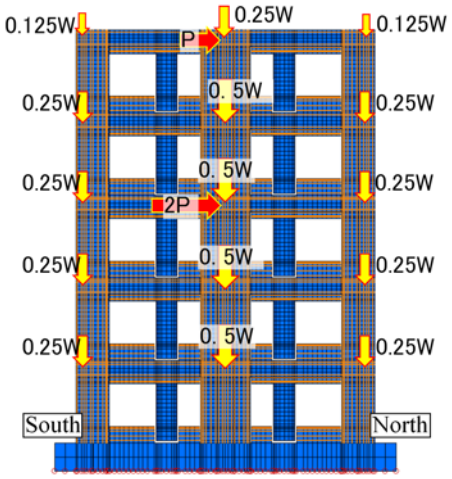

Figure 6. Finite element mesh and loading condition in *2D* finite element analysis

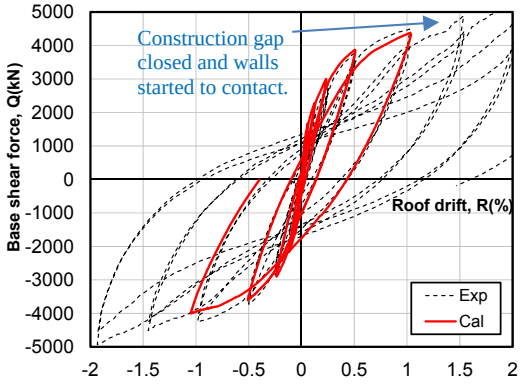

(a) Base shear force – roof level drift ratio relation

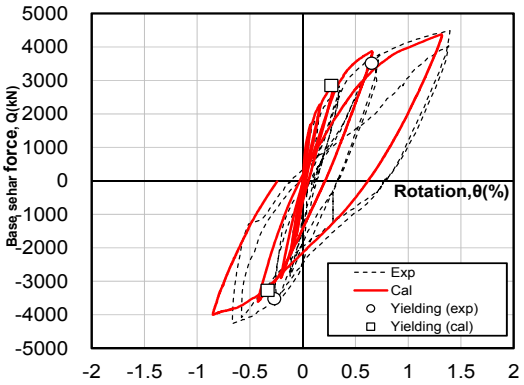

(b) Base shear – 1F north column rotation angle

Figure 7. Typical results of finite element analysis

Figure 7(a) shows base shear force – roof level drift relation. The numerical simulation agrees well with the experimental results. Figure 7(b) shows the base shear force – member rotation of the north column (1F). The rotation in experiment was obtained using displacement gages in Figure 3(c). The deformation of each member directly influences the simulation of crack performance and detailed measurement was conducted with special care. The simulated curve agreed relatively well with the experimental results in the positive side but did not agree very well in the negative side. The results for the beam (2F) and wing wall (1F) had similar trend although their plots are not shown due to space limitation.

3.2 Numerical simulation of flexural cracks

Most cracks were governed by flexure as can be seen in Figure 4 and Figure 5 and numerical simulation treated only flexural cracks. Some flexural-shear cracks existed at the end of beams and this effect was considered with conversion index, α , which is explained later. Treatment of shear cracking is also important but will be discussed elsewhere.

The column (1F) is used as an example to explain how to obtain spacing, width, and length of flexural cracks. Crack width was computed based on Eq. (1). It assumes that concrete itself does not deform and deformation of a member comes from crack openings. Hence, strain obtained from the finite element analysis represents effects of smeared cracks. Based on this assumption, the flexural crack width of a column can be obtained by integrating vertical tensile strain (ε_{zz}) over a crack spacing (s_{rm}). The crack spacing is based on Eq. (2) proposed in CEB-FIP Model Code (CEB-FIP 1978). Equation (2) is based on the condition that the number of cracks is saturated. The error of the equation was checked beforehand and turned out to be negligible after R=0.25%.

$$w_i = \int_{h_i - s_{rm}/2}^{h_i + s_{rm}/2} \varepsilon_{zz}\, dz \tag{1}$$

$$s_{rm} = 2\left(c_s + \frac{s_y}{10}\right) + k_1 k_2 \frac{d_{by}}{p_y} \tag{2}$$

where w_i and h_i are crack width and height of the i-th crack, ε_{zz} is vertical strain in vertical (z) direction, s_{rm} is crack spacing. Other notations in Eq. (2) should be referred to the original document.

Figure 8 shows accumulated crack width for the north column (1F) and the wing wall (1F). Crack width was accumulated from the top to the bottom of the column. The accumulated crack width at the bottom is close to the elongation measured by displacement gages, and elongation is expressed by the vertical break lines in the figure. Figure 8(a) and (c) shows variaions at the peaks at different drift cycles and (b) and (d) show those at the unloaded conditions. Solid circles on the expecimental curves show the location of actural cracks and those for analysis show simulated points with spacing s_{rm}. Each figure has comparisons between experimental and anlytical results for three drift levels at R=0.25%, 0.5% and 1%. Simulated variations for peak load agreed relatively well with experimental rusults for the column and wing wall. However, the agreement is not very good for residual crack width. If the total elongation of the tension fiber in analysis does not agree with exerimental results, the simulation does not agree with the experimental resutls. It should be noted that residual crack width was taken to be half of the peak crack width based on the AIJ guidelines (AIJ 2004) although this should take into account the effects of axial load.

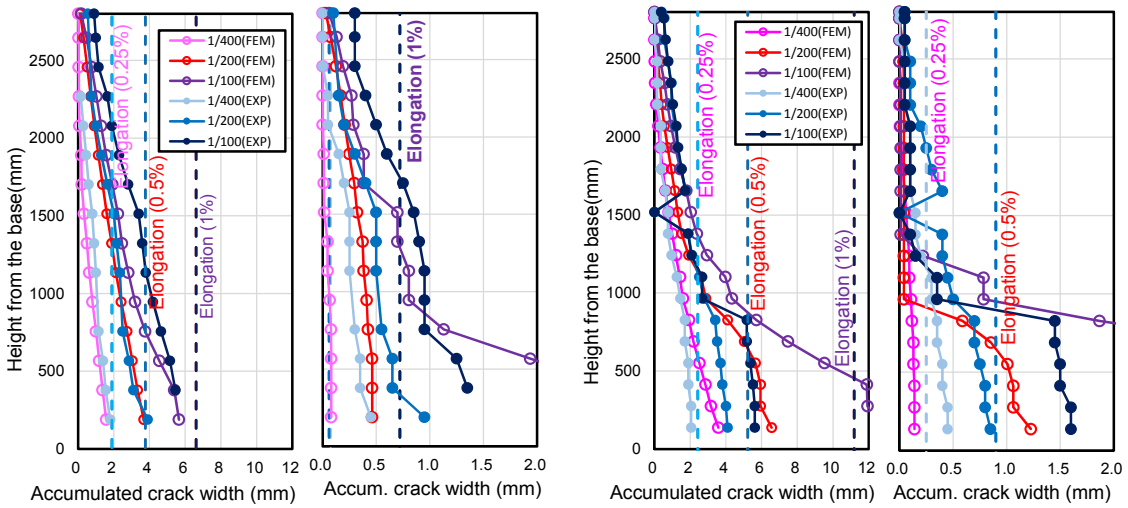

(a) North column (peak) (b) North column (residual) (c) North Wing wall (peak) (b) North Wing wall (residual)
Figure 8. Accumulated crack width distribution

Crack length was computed using analytical results of FEM as well. The crack was assumed visible when longitudinal tensile strain, ε_{zz}, exceeded the limit crack strain, ε_{cr}, in Eq. (3), that is, crack width exceeds $(\varepsilon_{cr} \cdot s_{rm})$. Based on this assumption, crack length at $z = h_i$ is computed using the longidinal tensile fiber strain of concrete from FEM.

$$\varepsilon_{cr} = 2\frac{f_t}{E_c} \tag{3}$$

$$L_h = \sum_{k=1}^{n}\left(D - x_{n(k)} - x_{cr(k)}\right) \tag{4}$$

$$L_f = \alpha L_h \tag{5}$$

$$\alpha = \alpha_1 \cdot \alpha_2 \tag{6}$$

$$\alpha_1 = \frac{L_{f(\exp)}}{L_v} \quad \text{(meandering effects)} \tag{7}$$

$$\alpha_2 = \frac{L_v}{L_h} \quad \text{(conversion from horizontal projection to diagonal length)} \tag{8}$$

Crack length was computed as shown in Figure 9. Crack lenght was computed at first peaks of each drift angle. Hence, the projectected crack length, L_h,was computed based on the strain distribution at peak points at the first cycle. Conversion index, α, was multiplied to obtain crack length, L_f, to take into the fact that cracks are not smooth nor horizontal. Index, α, was determined from the experimetal results and the values were 1.15, 1.28, and 1.51 for the column, wing wall, and beam.

Figure 10 shows crack ratio, β_L. Crack ratio, β_L, is the ratio of all crack length summation to the square root of surface area, A, and no-dimensional quantity as expressed by Eq. (9).

$$\beta_L = \frac{\sum L_f}{\sqrt{A}} \tag{9}$$

Based on the reference (JDPDA 2015), crack width is categorized into four classes of crack width $(0 \le w_{cr} \le 0.2mm,\ 0.2mm \le w_{cr} \le 1mm,\ \ 1\text{mm} \le w_{cr} \le 2mm\ \ w_{cr} \ge 2mm)$ and β_L for each category is expressed as a stack graph. Transition of crack ratio is well simulated up

to R=0.5% for the column and beam but not very well for R=1.0%. The simulation is not very good for wall because the crack width simulation is not very good.

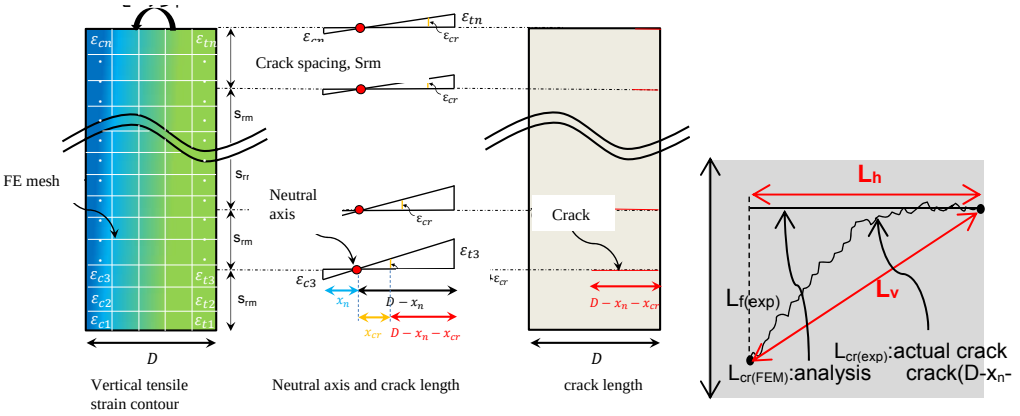

(a) Strain (ε_{zz}) distribution (b) Location of NA (c) horizontal crack length (d) Conversion to meandering crack

Figure 9. Calculation of crack length

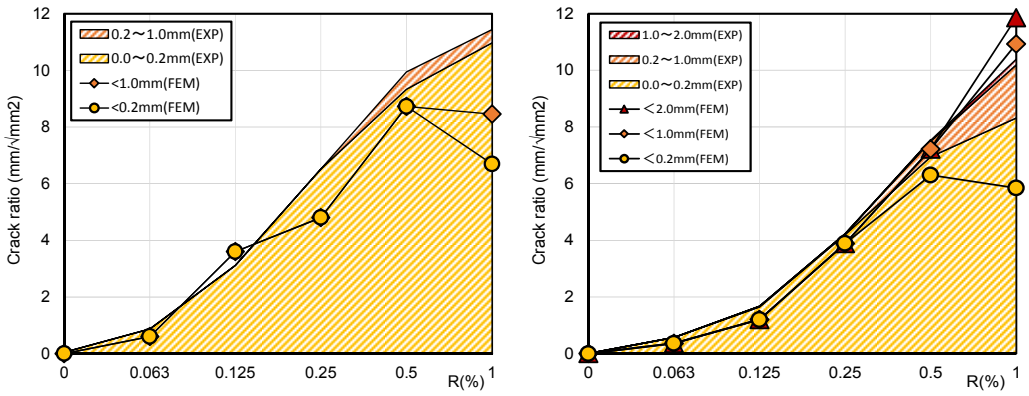

(a) North column (b) North beam

Figure 10. Variation of crack density

4 CONCLUSIONS

Cracks are one of the index to represent early stage damage of reinforced concrete structures. In order to assess damage state of real scale buildings, crack width, length and spacing were simulated for the real scale five story reinforced concrete building specimen tested in 2014 by post-processing the numerical results of finite element analysis.

- Accumulated crack width show that crack width and spacing were well simulated for peak points of each cycles. However, residual crack width was not well simulated.
- Crack length can be simulated by making some assumptions that concrete does not deform, visible crack is determined by limit strain.
- Computed rack ratio well simulated experiment results for different crack width categories.

The authors hope that simulation of crack features helps to evaluate early stage damage condition in higher precision. This work will fill the research gap of detailed evaluation of seismic performance of reinforced concrete buildings for minor to intermediate damage.

5 ACKNOWLEDGEMENT

This study was carried out by a joint study of National Technology Development Project of MLIT "Development of function sustaining technologies for buildings used as Disaster Prevention Bases" (2013 ～ 2016) and Priority Research Program of BRI Development on Seismic Design Method for Building with Post Earthquake Functional Use"(2013～2015). The efforts in measuring concrete cracking by Tokyo Institute of technology, Tokyo University of Science and Tohoku University are gratefully acknowledged. A part of this study was conducted as Scientific Research A (PI: Susumu Kono) of JSPS Grant-in-Aid program. Some financial support was also granted by the World Research Hub Initiative of the Institute of Innovative Research and the Collaborative Research Project of Materials and Structures Laboratory at Tokyo Institute of Technology.

6 REFERENCES

Architectural Institute of Japan, Guidelines for Performance Evaluation of Earthquake Resistant Reinforced Concrete Buildings (Draft), 2004.

CEB-FIP: Model Code for Concrete Structures, 15.2.3 Limit states of cracking, pp.156-160, 1978

Ciampi, V. et al.: Analytical Model for Concrete Anchorages of Reinforcing Bars Under Generalized Excitations, Report No. UCB/EERC-82/23, Univ. of California, Berkeley, Nov., 1982

Fukuyama, H.: Static Loading Test on A Full Scale Five Story Reinforced Concrete Building utilizing Wing Walls for Damage Reduction, Summaries of technical papers of Annual Meeting Architectural Institute of Japan. C-2, 2015, pp. 361-362.

ITOCHU Techno Solutions Corporation: Science and Engineering Systems Division: Final user's manual, 2016

Izumo J., Shima H., and Okamura H.: Analytical Model for Reinforced Concrete Panel Elements Subjected to In-Plane Forces, Concrete Research and Technology, Vol. 25 (1987), No. 9, Pp. 107-120

JBDPA (The Japan Building Disaster Prevention Association), Seismic Evaluation and Retrofit, 2015

Kabeyasawa T., Mukai T., Fukuyama H., et al.: A Full Scale Static Loading Test on Five Story Reinforced Concrete Building Utilizing Columns with Wing Walls, Journal of Structural and Construction Engineering, Transactions of AIJ, Vol. 81, 2016, No. 720, 313-322.

Kabeyasawa T., Mukai T., Fukuyama H., Suwada H., and Kato H.: Full-scale static loading test on a five story reinforced concrete building, 16th World Conference on Earthquake Engineering, Santiago Chile, January 9 – 13, 2017, Paper No. 1242

Kitamura F.: Damage evaluation of five-story building by nonlinear finite element analysis, Master thesis of Tokyo Instute of Technology, 2017.

MLIT (Ministry of Land, Infrastructure): Transportation and Tourism (MLIT): The 2015 guidelines of structural design technology of buildings, 2015.

Naganuma K.: Stress – strain relationship for concrete under triaxial compression, Journal of Structural and Construction Engineering, Transactions of AIJ, 1995, No. 474, pp. 163-170.

Sato Y. and Naganuma K.: Crack Width Analysis Using Smeared-Crack-Based FEM: Part 8, Summaries of tech. papers of Annual Meeting Architectural Inst. of Japan. C-2, 2011, pp. 241-242.

Maeda M., Nakano Y., and Lee K.: Post-Earthquake Damage Evaluation for R/C Buildings based on Residual Seismic Capacity. Proc. of 13 World Conference on Earthquake Engineering, (2004), 1179-